Received: 11 November 2021 | Revised: 18 March 2022 | Accepted: 4 April 2022
DOI: 10.1002/cta.3301

ORIGINAL PAPER

WILEY

MONA—A magnetic oriented nodal analysis for electric circuits

Vsevolod Shashkov[1] | **Idoia Cortes Garcia**[2] | **Herbert Egger**[3]

[1]TU Darmstadt, Darmstadt, Germany
[2]Eindhoven University of Technology, Eindhoven, The Netherlands
[3]Johannes Kepler University Linz and Johann Radon Institute for Computational and Applied Mathematics, Linz, Austria

Correspondence
Vsevolod Shashkov, TU Darmstadt, Dolivostr. 15, 64293 Darmstadt, Germany.
Email: shashkov@mathematik.tu-darmstadt.de

Funding information
German Science Foundation (DFG), Grant/Award Number: TRR361; Austrian Science Fund (FWF), Grant/Award Number: SFB F90-N; Center for Computational Engineering at TU Darmstadt

Abstract
The modified nodal analysis (MNA) is probably the most widely used formulation for the modeling and simulation of electric circuits. Its conventional form uses electric node potentials and currents across inductors and voltage sources as unknowns, thus taking an *electric viewpoint*. In this paper, we propose an alternative *magnetic oriented nodal analysis* (MONA) for electric circuits, which is based on magnetic node potentials and charges across capacitors and voltage sources as the primary degrees of freedom, thus giving direct access to these quantities. The resulting system has the structure of a generalized gradient system which immediately ensures passivity in the absence of sources. A complete index analysis is presented showing regularity of the magnetic oriented formulation under standard topological conditions on the network interconnection. In comparison to conventional MNA, the differential-algebraic index of MONA is smaller by one in most cases which facilitates the numerical solution. Some preliminary numerical experiments are presented for illustration of the feasibility and stability of the new approach.

KEYWORDS
charge-flux oriented formulation, differential-algebraic equations, electrical circuits, index analysis, modified nodal analysis

1 | INTRODUCTION

The modeling and simulation of electric devices is one of the fundamental problems in electrical engineering. Very often the system dynamics can be described as an electric interconnection network,[1–4] by equivalent electric or magnetic circuit models,[5–7] or by combinations of circuit and field equations.[8–12] Since its introduction in the mid 1970s,[13] the *modified nodal analysis* (MNA) has become the industry standard for electric circuit design and the simulation. For an overview and further references, we refer to previous studies.[2,4,14,15] In compact form, the governing equations read

$$A_C\frac{d}{dt}q(A_C^\top e)+A_Rg(A_R^\top e)+A_Li_L+A_Vi_V=-A_Ii_{src}, \tag{1}$$

$$\frac{d}{dt}\phi(i_L) - A_L^\top e = 0, \tag{2}$$

$$-A_V^\top e = -v_{src}. \tag{3}$$

Here, e denotes the vector of electric node potentials, i_L, i_V are the currents through inductors and voltage sources, and i_{src}, v_{src} are prescribed source terms. The interconnection of the individual devices is encoded in the partial incidence matrices A_x, with x characterizing the type of the circuit element. The characteristics of capacitors, inductors and resistors are described by the nonlinear device functions $q(v_C), \phi(i_L), g(v_R)$ with $v_x = A_x^\top e$ denoting the voltages across elements. See, for example, previous studies,[2,4,14] for details of the modeling and notation.

The nonlinear relations for inductors and capacitors may also be expressed as

$$\frac{d}{dt}q(v_C) = C(v_c)\frac{d}{dt}v_c, \quad \frac{d}{dt}\phi(i_L) = L(i_L)\frac{d}{dt}i_L, \tag{4}$$

with $C(v_C)$ and $L(i_L)$ denoting the more common differential capacitance and inductance matrices, respectively. These matrices are related to the Hessians of corresponding electric and magnetic energy functionals and, consequently, they can be assumed symmetric and positive definite; see Sections 2 and 3 for details. The device functions for resistors, on the other hand, are assumed to satisfy

$$g(v_R) = (g_1(v_{R,1}), ..., g_m(v_{R,m}))^\top \text{ with } \ g_j'(v_j) > 0, g(0) = 0. \tag{5}$$

This means that the current $i_{R,j} = g_j(v_{R,j})$ in the jth resistor depends monotonically on the applied voltage and further implies that the Jacobian $\partial g(v_R)/\partial v_R$ is positive definite; see previous studies.[4,16] For our analysis later on, we will utilize the slightly more general condition

$$g(v_R) = G(v_R)v_R \tag{6}$$

with generalized conductivity matrix $G(v_R)$ assumed to be symmetric and positive semi-definite and smoothly depending on its arguments. Substituting the identities (4) into (1)–(3) leads to the *conventional form* of the MNA which has the formal structure of a *port-Hamiltonian system*.[17] Together with (5) or (6) this automatically guarantees passivity of the system; see, for example, previous studies[18,19] and Section 2.

A mathematical subtelty arising in the context of circuit modeling is the differential-algebraic nature of the governing systems.[20,21] In fact, the research in differential-algebraic equations and their numerical solution has been stimulated substantially for many years by applications in electronic circuits; see previous studies[22–24] for an introduction and further references. It is now well understood that for consistent initial conditions and appropriate device characteristics

(a1) the system (1)–(4) is well-posed and has index $\nu \leq 2$ if the circuit contains neither loops of voltage sources nor cutsets of current sources.

Moreover, one can show that

(a2) the index is $\nu \leq 1$ if the circuit contains neither loops of capacitors and voltage sources nor cutsets of inductors and current sources;

see previous work[3,25–27] for details and proofs. The condition in (a2) could in fact be slightly relaxed, for example, loops consisting of capacitors only could be allowed; cf. Günther et al.[18] (Remark 20) for details. Let us note that the conditions in (a1) and (a2) are purely topological, that is, concerning only the interconnection of components, and they can therefore be formulated as algebraic conditions on the partial incidence matrices A_x, as worked out in previous studies.[2,25,27] This allows for a systematic *projection-based analysis*[20,28] and different index concepts have been successfully employed to prove (a1)–(a2) and generalizations; we refer to previous studies[14,16,28] for further results and references.

Besides their analytical peculiarities, electric circuit equations also pose various challenges for the numerical solution. Due to the differential-algebraic nature, implicit time stepping schemes have to be used.[22–24] While passivity on the discrete level can be proven rigorously for the implicit Euler method and related variational time discretization schemes of higher order,[29] strict passivity may in general be lost through discretization by standard single or multistep schemes. In the presence of strong nonlinearities, even well-established second order schemes, like the trapezoidal rule or BDF-2 method may run into stability problems. A common practice in industry therefore is to use low order time integration schemes in general and eventually fall back to the implicit Euler method in case of stability issues; we refer to Günther et al.[4] (Ch. 10,11) for details.

Another somehow related difficulty is that the nonlinear differential relations (4) for device characteristics, which were employed in the derivation of the conventional form of the MNA, can in general not be reproduced exactly on the discrete level. As a consequence, charge conservation may be lost after discretization and simulated magnetic fluxes may be inconsistent. A possible remedy is to introduce extra variables

$$q_C = q(v_C), \quad \phi_L = \phi(i_L) \tag{7}$$

for the electric charges and magnetic fluxes which together with (1)–(3) leads to the *charge/flux oriented MNA*; see[4] for an overview. The assertions (a1) and (a2) can be verified also for this extended formulation,[25] but some additional modifications are required to reveal the port-Hamiltonian structure.[18] Such extensions typically involve substantially more unknowns than the conventional MNA, in particular, if many capacitative or inductive devices are present.

Let us emphasize that all formulations mentioned so far involve the electric node potentials e as the primary unkowns and could therefore be called *electric oriented* nodal analyses. In this paper, we take an alternative *magnetic viewpoint* and introduce a *magnetic oriented* nodal analysis (MONA) for the modeling and simulation of electric circuits. In its compact form, the resulting formulation reads

$$A_R g\left(A_R^\top \frac{d}{dt}\psi\right) + A_C \frac{d}{dt} q_C + A_V \frac{d}{dt} q_V + A_L i(A_L^\top \psi) = -A_I i_{src}, \tag{8}$$

$$-A_C^\top \frac{d}{dt}\psi + v(q_C) = 0, \tag{9}$$

$$-A_V^\top \frac{d}{dt}\psi = -v_{src}. \tag{10}$$

Here, ψ denotes a vector of magnetic node potentials and q_C, q_V are the displaced charges at capacitors and voltage sources. The formulation clearly has a great similarity with the MNA, allowing to reuse available implementations, but it also has some subtle differences. Access to the magnetic flux linkages and electric node potentials is now available through

$$\phi_L = A_L \psi, \quad e = \frac{d}{dt}\psi, \tag{11}$$

from which voltages and currents can be derived like in the electric based nodal analysis above. While the conductance relation $g(v_C) = G(v_C) v_C$ is the same as in (1), the device characteristics of inductors and capacitors are now described by

$$i(\phi_L) = \nabla \epsilon_L(\phi_L), \quad v(q_C) = \nabla \epsilon_C(\phi_C) \tag{12}$$

with $\epsilon_L(\cdot), \epsilon_C(\cdot)$ denoting magnetic and electric energy functionals, respectively. To draw the connection with the previous models, we may differentiate Equation (12) to see that

$$\frac{d}{dt} i(\phi_L) = \nabla^2 \epsilon_L(\phi_L) \frac{d}{dt}\phi_L, \quad \frac{d}{dt} v(q_C) = \nabla^2 \epsilon_C(q_C) \frac{d}{dt} q_C. \tag{13}$$

A quick comparison with the relations (4) reveals that the Hessians $\nabla^2\epsilon_L(\phi_L)=L(i(\phi_L))^{-1}$ and $\nabla^2\epsilon_C(q_C)=C(v(q_C))^{-1}$ are directly linked to the differential inductance and capacitance matrices employed before. The derivation of the system (1)–(3) is based on the very same principles as the new model (8)–(10), and the electric and magnetic viewpoints are therefore mutually equivalent allowing to model the same circuits.

Let us also note that in the magnetic oriented formulation (8)–(11), the resistive terms and the interconnection structure affect the time derivatives, in contrast to (1)–(3), where they involve only the lowest order terms. The system (8)–(11) therefore has a different geometric structure as the MNA, namely that of a *generalized gradient system*, which however immediately allows to guarantee again passivity of the system; see previous studies[30,31] and Section 3 below. We will further show that for consistent initial conditions and under appropriate assumptions on the device characteristics

(b1) the system (8)–(10) is well-posed and has index $\nu\leq 1$ if the circuit contains neither loops of voltage sources nor cutsets of current sources;
(b2) the index is $\nu=0$ if the circuit contains neither loops of capacitors and voltage sources nor cutsets of inductors and current sources.

Note that the conditions in (b1) and (b2) are exactly the same as those employed in the assertions (a1) and (a2) before, that is, the new magnetic oriented formulation is as flexible and general as the electric one. In comparison to the conventional MNA, the proposed magnetic oriented formulation leads to a system of a smaller index in most cases, which alleviates the numerical solution to some extent. Apart from this numerical advantage, a benefit of our approach is the direct access to the charges q_C, q_V and flux linkages $\phi_L=A_L^\top\psi$, which might be of particular interest in certain applications, for example, if many energy storing elements are present in the circuit. A disadvantage of the magnetic oriented formulation, on the other hand, seems to be that access to electric quantities, like electric potentials and branch currents, is somewhat indirect, for example, via $e=\frac{d}{dt}\psi$, which however can be realized exactly also on the discrete level, if appropriate time stepping is applied.[30] Before the introduction, let us mention that an alternative *branch-based* formulation using charges and fluxes across capacitors and inductors was recently proposed in Nedialkov et al[32] and shown to always lead to an index ≤ 1. This approach however requires some additional algebraic pre-processing not needed in our method.

The remainder of the manuscript is organized as follows: in Section 2, we introduce our notation and recall some basic facts about the conventional electric oriented nodal analysis. The new magnetic oriented formulation is then derived in Section 3 and a short proof of its passivity is provided. Section 4 is concerned with the index analysis of MONA and contains the proof of assertions (b1) and (b2). Some preliminary numerical results for our method and a brief comparison with the conventional MNA are presented in Section 5.

2 | BASIC NOTATION AND A REVIEW OF MNA

We consider a directed and connected graph with N_n nodes and N_b branches. Its interconnection structure is described by the *incidence matrix*$A\in\mathbb{R}^{N_n\times N_b}$ defined as

$$A_{ij}=\begin{cases}1 & \text{if branch } j \text{ leaves node } i,\\ -1 & \text{if branch } j \text{ enters node } i,\\ 0 & \text{else.}\end{cases}$$

We use the same letter A to denote the reduced incidence matrix which results from eliminating one row corresponding to a grounded node. Kirchhoff's current law and the definition of the voltages across elements can then be expressed as

$$Ai=0 \ \text{ and } \ v=A^\top e, \tag{14}$$

with i, v, and e denoting the vectors of branch currents, branch voltages, and node potentials, respectively. We consider circuits consisting of resistors, inductors, capacitors, and independent current and voltage sources. This allow to split

$$A = [A_C, A_L, A_R, A_V, A_I]$$

with A_x representing the partial incidence matrix of the elements of type x. In a similar manner, we split the vectors of currents and voltages and denote by i_x and v_x the corresponding sub-vectors. The system (14) is complemented by constitutive relations

$$i_C = C(v_C)\frac{d}{dt}v_C, \quad v_L = L(i_L)\frac{d}{dt}i_L, \quad \text{and} \quad i_R = G(v_R)v_R, \tag{15}$$

which describe the device characteristics of capacitors, inductors, and resistors, respectively. The matrices $C(v_C), L(i_L)$, and $G(v_R)$ are the differential capacitance, differential inductance, and the generalized conductance, respectively, and they are assumed to be symmetric positive definite and to depend smoothly on their arguments. The currents $i_I = i_{src}$ and voltages $v_V = v_{src}$ denote the input to the system. Substituting (15) into (14) leads to the system

$$A_C C(A_C^\top e)A_C^\top \frac{d}{dt}e + A_R G(A_R^\top e)A_R^\top e + A_L i_L + A_V i_V = -A_I i_{src} \tag{16}$$

$$L(i_L)\frac{d}{dt}i_L - A_L^\top e = 0 \tag{17}$$

$$-A_V^\top e = -v_{src} \tag{18}$$

which is the conventional form of the modified nodal analysis[13]; also see previous studies.[2,4,25] In the following, we briefly recall the most important results of its analysis.

Energy balance and passivity. We start with deriving the basic energy–dissipation identity. To this end, let $\epsilon_L(\phi_L)$ and $\epsilon_C(q_C)$ denote the energy stored in inductors and capacitors, respectively, and recall[4,25] that

$$\nabla\epsilon_L(\phi_L) = i_L, \quad \nabla\epsilon_C(q_C) = v_C.$$

With these identities and expressing $\phi_L = \phi(i_L)$ and $q_C = q(v_C)$, we immediately obtain

$$\begin{aligned}\frac{d}{dt}(\epsilon_C(q(v_C)) + \epsilon_L(\phi(i_L))) &= \langle \nabla\epsilon_C(q(v_C)), \frac{d}{dt}q(v_C)\rangle + \langle \nabla\epsilon_L(\phi(i_L)), \frac{d}{dt}\phi(i_L)\rangle \\ &= \langle v_C, C(v_C)\frac{d}{dt}v_C\rangle + \langle i_L, L(i_L)\frac{d}{dt}i_L\rangle,\end{aligned}$$

where we used (4) in the second step. Here and below, $\langle a,b\rangle = b^\top a$ is the Euclidean inner product. After substituting $v_C = A_V^\top e$, one can see that the result amounts to the first terms in (16)–(17) multiplied by $e^\top$ and $i_L^\top$ from the left. Inserting these equations and rearranging the terms thus leads to

$$\begin{aligned}\frac{d}{dt}(\epsilon_C(q(v_C)) + \epsilon_L(\phi(i_L))) &= -\langle e, A_R^\top G(v_R)A_R^\top e + A_L i_L + A_V i_V + A_I i_{src}\rangle + \langle i_L, A_L^\top e\rangle \\ &= -\langle e, A_R G(v_R)A_R^\top e\rangle - \langle A_I^\top e, i_{src}\rangle - \langle i_V, v_{src}\rangle,\end{aligned}$$

where we used (18) and some elementary algebraic manipulations in the last step. This identity states that the energy of the system changes only by dissipation in resistors and supply or loss through voltage and current sources. In particular, when $i_{src} = v_{src} = 0$, we obtain passivity of the system.

Index analysis. As a second step, let us recall some basic facts about the index analysis of the MNA equations. Recall that $L(i_L)$ and $C(v_C)$ are assumed symmetric and positive definite matrices that depend smoothly on their arguments. Moreover, $\partial g(v_R)/\partial v_R$ was assumed positive definite. Under these assumptions, one has the following result.

Lemma 1. Assume that

$$N([A_R, A_C, A_V, A_L]^\top) = 0 \quad \text{and} \quad N(A_V) = 0. \tag{A1}$$

Then (16)–(18) is a regular system of DAEs with index $\nu \le 2$. If additionally

$$N([A_R, A_C, A_V]^\top) = 0 \quad \text{and} \quad N([A_C, A_V]) = 0. \tag{A2}$$

Then the system is again regular and of index $\nu \le 1$.

Detailed proofs can be found, for example, in previous studies.[16,25,27] Let us note that the algebraic conditions (A1)–(A2) are equivalent to the topological conditions in (a1)–(a2) mentioned in the introduction; for details, see Estévez Schwarz and Tischendorf (Theorem 2.2)[25] and Günther et al. (Remark 17).[18] Similar to assertion (a2) the condition (A2) could again be slightly relaxed for the second statement.

3 | THE MAGNETIC ORIENTED NODAL ANALYSIS

By Faraday's law, the voltage induced by a time varying magnetic flux through a wire loop is given by $v_L = \frac{d}{dt}\phi_L$. Integrating this expression and using $v_L = A_L^\top e$ leads to $\phi_L(t) = A_L^\top \int_0^t e(\tau)d\tau + \phi_L(0)$. We now introduce a *magnetic node potential* by $\psi(t) = \psi_0 + \int_0^t e(\tau)d\tau$, with initial value satisfying $\phi_L(0) = A_L^\top \psi_0$. This construction implies

$$e = \frac{d}{dt}\psi, \quad \phi_L = A_L^\top \psi. \tag{19}$$

In addition, we consider an integral form of charge conservation by introducing generalized charges $q_x(t) = q_{x,0} + \int_0^t i_x(\tau)d\tau$. This allows us to compute the currents and voltages

$$i_C = \frac{d}{dt}q_C, \quad i_V = \frac{d}{dt}q_V \quad \text{and} \quad v_C = A_C^\top \frac{d}{dt}\psi, \quad v_V = A_V^\top \frac{d}{dt}\psi \tag{20}$$

across capacitors and voltage sources, respectively. Inserting these expressions in Kirchhoff's current law (14) and adding equations $v_C = v(q_C)$ and $v_V = v_{src}$ for the voltages across capacitors and voltage sources now immediately leads to the Equations 8–(10). Employing the relations $g(v_R) = G(v_R)v_R$ and (12) for the device characteristics, we arrive at

$$A_R G\left(A_R^\top \frac{d}{dt}\psi\right) A_R^\top \frac{d}{dt}\psi + A_C \frac{d}{dt}q_C + A_V \frac{d}{dt}q_V = -A_L \nabla \epsilon_L(A_L^\top \psi) - A_I i_{src} \tag{21}$$

$$-A_C^\top \frac{d}{dt}\psi = -\nabla \epsilon_C(q_C) \tag{22}$$

$$-A_V^\top \frac{d}{dt}\psi = -v_{src}, \tag{23}$$

which can be considered as the magnetic oriented formulation of (16)–(18). Let us note that the electric and magnetic oriented formulations are derived on the basis of the same physical principles and they can be transformed into each other.

Energy balance and passivity. As a first step of our analysis, we derive a basic energy-dissipation identity. By formal differentiation and noting that $\phi_L = A_L^\top \psi$, we see that

$$\frac{d}{dt}(\epsilon_L(\phi_L)+\epsilon_C(q_C)) = \langle \nabla\epsilon_L(\phi_L), A_L^\top \frac{d}{dt}\psi\rangle + \langle \nabla\epsilon_C(q_C), \frac{d}{dt}q_C\rangle.$$

Apart from the source current, this amounts to the right hand sides of (21)–(22) multiplied by $\frac{d}{dt}\psi^\top$ and $\frac{d}{dt}q_C^\top$ from the left. Inserting the equations therefore gives

$$\begin{aligned}\frac{d}{dt}(\epsilon_L(\phi_L)+\epsilon_C(q_C)) &= -\langle A_R G\left(A_R^\top \frac{d}{dt}\psi\right)A_R^\top \frac{d}{dt}\psi + A_C\frac{d}{dt}q_C + A_V\frac{d}{dt}q_V + A_I i_{src}, \frac{d}{dt}\psi\rangle \\ &\quad + \langle A_C^\top \frac{d}{dt}\psi, \frac{d}{dt}q_C\rangle = -\langle A_R G\left(A_R^\top \frac{d}{dt}\psi\right)A_R^\top \frac{d}{dt}\psi, \frac{d}{dt}\psi\rangle - \langle i_{src}, v_I\rangle - \langle i_V, v_{src}\rangle,\end{aligned}$$

where we used (23) and some elementary algebraic manipulations in the last step. The energy of the system can therefore again only change due to dissipation in the resistors and power supplied or drawn through current and voltage sources. In particular, the system is passive in the absence of source terms.

4 | INDEX ANALYSIS

As a second step of our analysis, we now consider in detail the differential-algebraic index of the system under consideration. For ease of notation, we choose $i_{src}=v_{src}=0$ and then rewrite the system (21)–(23) in compact form

$$\begin{pmatrix} A_R G^\psi A_R^\top & A_C & A_V \\ -A_C^\top & & \\ -A_V^\top & & \end{pmatrix} \frac{d}{dt}\begin{pmatrix}\psi \\ q_C \\ q_V\end{pmatrix} = -\begin{pmatrix} A_L\nabla\epsilon_L(A_L^\top\psi) \\ \nabla\epsilon_C(q_C) \\ 0\end{pmatrix} \tag{24}$$

We use $G^\psi = G\left(A_R^\top \frac{d}{dt}\psi\right)$ to abbreviate the solution dependent conductivity matrix in the following. In addition, we assume regular device characteristics, which can be stated as

$$G^\psi \text{ symmetric and positive definite and } \epsilon_L,\, \epsilon_C \text{ are strictly convex,} \tag{A0}$$

with all functions depending smoothly on their arguments. Let us note that these were the standard assumptions also for the investigation of the MNA summarized in the previous section. Under the algebraic conditions of Lemma 1, we then obtain the following result.

Theorem 1. Let (A0) hold and assume that

$$N([A_R, A_C, A_V, A_L]^\top) = 0 \quad \text{and} \quad N(A_V) = 0. \tag{A1}$$

Then the system (24) is a regular DAE of index $\nu = 1$. If in addition to (A1) also

$$N([A_R, A_C, A_V]^\top) = 0 \quad \text{and} \quad N([A_C, A_V]) = 0 \tag{A2}$$

holds, then (24) is a regular DAE of index $\nu = 0$, that is, an ordinary differential equation.

For the proof of this theorem, we utilize the following basic result of linear algebra.

Lemma 2: Brezzi's splitting lemma[33]. A matrix $\begin{pmatrix} K & B^\top \\ -B & 0\end{pmatrix}$ is regular, if and only if

$$N(B^\top)=0 \quad \text{and} \quad N(K)\cap N(B)=0.$$

Proof of Theorem 1. We start with the second assertion, for which we show that the matrix in front of the time derivative in (24) is regular. This matrix has the structure of the previous lemma with $B=[A_C,A_V]^\top$ and $K=A_R G^\psi A_R^\top$. By assumption (A2), we see that

$$N(B^\top)=N([A_C,A_V])=0,$$

which is the first condition of Breezi's splitting lemma. Furthermore

$$\langle K\psi,\psi\rangle=\langle G^\psi A_R^\top\psi, A_R^\top\psi\rangle\geq\gamma\|A_R^\top\psi\|^2$$

with some $\gamma>0$, since G^ψ is positive definite by assumption (A0). By assumption (A2), we further see that $N(A_R^\top)\cap N([A_C,A_V]^\top)=N([A_R,A_C,A_V]^\top)=0$ and hence

$$\langle K\psi,\psi\rangle\neq 0 \quad \text{for all} \psi\in N(B), \psi\neq 0,$$

which proves the second assertion of Brezzi's splitting lemma. Hence, the system (24) is an implicit ODE, that is, a regular DAE with index $\nu=0$.

We now turn to the first assertion of the lemma, for which we use a typical projection-based analysis.[28] If the conditions (A2) are not valid, we simply split the vector spaces of magnetic potentials ψ and charges $q=(q_C,q_V)$ into

$$\begin{aligned} V_\psi &= N([A_R,A_C,A_V]^\top)\oplus N([A_R,A_C,A_V]^\top)^\perp \\ V_q &= N([A_C,A_V])\oplus N([A_C,A_V])^\perp. \end{aligned}$$

By choosing orthogonal bases for the corresponding subspaces, we can thus decompose

$$\psi=Q_1\psi_1+Q_2\psi_2 \quad \text{and}\ q=P_1q_1+P_2q_2.$$

with $Q=[Q_1,Q_2]$ and $P=[P_1,P_2]$ orthonormal matrices. Moreover, $[A_R,A_C,A_V]^\top Q_1=0$ and $[A_C,A_V]P_1=0$, while $[A_R,A_C,A_V]^\top Q_2$ and $[A_C,A_V]P_2$ have trivial nullspace. The second splitting can also be written component-wise as

$$\begin{pmatrix} q_C \\ q_V \end{pmatrix}=\begin{pmatrix} P_{1,C} \\ P_{1,V} \end{pmatrix}q_1+\begin{pmatrix} P_{2,C} \\ P_{2,V} \end{pmatrix}q_2.$$

We now multiply the system (24) from left by blkdiag$(Q^\top,P^\top)$ and use the above expansions for ψ and $q=(q_c,q_v)$, which leads to the equivalent form

$$\begin{pmatrix} 0 & 0 & 0 & 0 \\ 0 & \tilde{K} & 0 & \tilde{B}^\top \\ 0 & 0 & 0 & 0 \\ 0 & -\tilde{B} & 0 & 0 \end{pmatrix}\frac{d}{dt}\begin{pmatrix} \psi_1 \\ \psi_2 \\ q_1 \\ q_2 \end{pmatrix}=-\begin{pmatrix} Q_1^\top A_L\nabla\epsilon_L(A_L^\top(Q_1\psi_1+Q_2\psi_2)) \\ Q_2^\top A_L\nabla\epsilon_L(A_L^\top Q_1\psi_1+Q_2\psi_2)) \\ P_{1,C}^\top\nabla\epsilon_C(P_{1,C}q_1+P_{2,C}q_2) \\ P_{2,C}^\top\nabla\epsilon_C(P_{1,C}q_1+P_{2,C}q_2) \end{pmatrix} \tag{25}$$

with $\tilde{K}=Q_2^\top A_R G^\psi A_R^\top Q_2$ and $\tilde{B}^\top=(Q_2^\top[A_C,A_V]P_2)$. By rearrangement of variables and equations, the system can then be written compactly as a Hessenberg system

$$M^{\psi}\frac{d}{dt}y = f(y,z) \tag{26}$$

$$0 = g(y,z) \tag{27}$$

with differential and algebraic variables $y=(\psi_2, q_2)$ and $z=(\psi_1, q_1)$, and leading matrix

$$M^{\psi} = \begin{pmatrix} \tilde{K} & \tilde{B}^{\top} \\ -\tilde{B} & 0 \end{pmatrix}.$$

We first show that this matrix is regular. By construction $N(\tilde{B}^{\top}) = 0$, which already yields the first condition of Brezzi's splitting lemma. Next observe that

$$N(\tilde{B}) = N(P_2^{\top}[A_C, A_V]^{\top}Q_2) = N([A_C, A_V]^{\top}Q_2).$$

Since G^{ψ} is regular by assumption (A0), we can thus deduce that

$$N(\tilde{K}) \cap N(\tilde{B}) = N(A_R^{\top}Q_2) \cap N([A_C, A_V^{\top}]Q_2) = N([A_R, A_C, A_V]^{\top}Q_2) = 0,$$

by definition of Q_2, which yields the second assertion of Breezi's splitting lemma. Thus the matrix M^{ψ} is regular. Let us now have a closer look on the algebraic constraint

$$0 = g(y,z) := \begin{pmatrix} Q_1^{\top}A_L\nabla\epsilon_L(A_L^{\top}(Q_1\psi_1 + Q_2\psi_2)) \\ P_{1,C}^{\top}\nabla\epsilon_C(P_{1,C}q_1 + P_{2,C}q_2) \end{pmatrix}$$

Using the chain rule, we see that

$$D_z g(y,z) = \begin{pmatrix} Q_1^{\top}A_L\nabla^2\epsilon_L(v_L)A_L^{\top}Q_1 & 0 \\ 0 & P_{1,C}^{\top}\nabla^2\epsilon_C(q_C)P_{1,C} \end{pmatrix} \tag{28}$$

with $v_L = A_L^{\top}(Q_1\psi_1 + Q_2\psi_2)$ and $q_C = P_{1,C}q_1 + P_{2,C}q_2$. Using assumption (A0), the two Hessians $L^{-1} = \nabla^2\epsilon_L(v_L)$ and $C^{-1} = \nabla^2\epsilon\epsilon_C(q_C)$ of the energy functionals can be seen to be symmetric and positive definite. Since Q_1 spans $N([A_R, A_C, A_V]^{\top})$, we further conclude from condition (A1) that $N(A_L^{\top}Q_1) = 0$, and hence, the upper left matrix in (28) is symmetric and positive definite. From the condition $N(A_V) = 0$, we further deduce that $(0, q_V) \in N([A_C, A_V])$ already implies $q_V = 0$. This shows that the matrix $P_{1,C}$ is injective, and hence, the lower right matrix is again symmetric and positive definite. Therefore, the Jacobian $D_z g(y,z)$ is regular, and as a consequence, the above Hessenberg system is a regular DAE of index $\nu = 1$. Since this system was obtained from (24) by algebraic equivalence transformation, the same is true for the original system.

Summary. Let us briefly summarize the theoretical observations of this section: under standard assumptions, the proposed magnetic oriented nodal analysis (MONA) is passive and a regular system of differential-algebraic equations. In comparison to conventional MNA or the charge-flux based formulations of Günther et al,[18] the index is typically smaller by one.

5 | NUMERICAL ILLUSTRATION

We now present numerical results for two simple test problems which demonstrate the stability and performance of MONA and highlight some possible advantages in comparison with the conventional modified nodal analysis.

Example 1: An Index-2 problem. In our first example, which is taken from Günther et al. (Ch. 10),[4] we consider an electric circuit containing a CV-loop; see Figure 1 for an illustration. The conventional MNA therefore leads to an index-2 problem, while according to Theorem 1 the MONA approach results in a system with index 1. The circuit contains only capacitors, resistors and one voltage source, and the network topology is described by following partial incidence matrices

$$A_C = \begin{pmatrix} 1 & 0 & 0 \\ -1 & 1 & 0 \\ 0 & 0 & 1 \end{pmatrix}, \quad A_R = \begin{pmatrix} 1 & 0 & 0 \\ 0 & 1 & 1 \\ 0 & 0 & -1 \end{pmatrix} \quad \text{and} \quad A_V = \begin{pmatrix} 1 \\ 0 \\ 0 \end{pmatrix}.$$

For ease of presentation, we consider linear constitutive equations with $C_i = 1$ and $R_i = 1$ for $i = 1,2,3$ and denote by $C = G = I_3$ the identity matrices of dimension 3. The conventional MNA formulation then leads to the following system

$$\begin{pmatrix} A_C C A_C^T & 0 \\ 0 & 0 \end{pmatrix} \frac{d}{dt} \begin{pmatrix} e \\ i_V \end{pmatrix} + \begin{pmatrix} A_R G A_R^T & A_V \\ -A_V^T & 0 \end{pmatrix} \begin{pmatrix} e \\ i_V \end{pmatrix} = \begin{pmatrix} 0 \\ -v_{src}(t) \end{pmatrix}$$

while the magnetic oriented scheme obtained by MONA reads

$$\begin{pmatrix} A_R G A_R^T & A_C & A_V \\ -A_C^T & 0 & 0 \\ -A_V^T & 0 & 0 \end{pmatrix} \frac{d}{dt} \begin{pmatrix} \psi \\ q_C \\ q_V \end{pmatrix} + \begin{pmatrix} 0 & 0 & 0 \\ 0 & C^{-1} & 0 \\ 0 & 0 & 0 \end{pmatrix} \begin{pmatrix} \psi \\ q_C \\ q_V \end{pmatrix} = \begin{pmatrix} 0 \\ 0 \\ -v_{src}(t) \end{pmatrix}.$$

Due to our choice of the constitutive equations, both systems are linear and time-invariant.

In Figure 2, we display the electric solution components obtained by numerical solution of the two equations by the trapezoidal rule (TR) with a fixed time step $\tau = 0.1$ and for $v_{src}(t) = \sin(\pi t)$. For our simulations, we chose trivial initial conditions, which are consistent with the algebraic constraint caused by the voltage source. This suffices to guarantee stability for the index-1 formulation obtained by MONA. The MNA system, on the other hand, has index 2 and a *hidden constraint* arises, which is not satisfied by our choice of initial conditions and causes large oscillations in the algebraic solution component. Let us note that this weak instability could be cured by an appropriate initialization phase, for example, by performing the first time step with the implicit Euler method. If we choose the source term $v_{src}(t) = \cos(t)$ inconsistent with the trivial initial values, then the TR-discretization of the MNA formulation leads to strong instabilities, which require a longer initialization phase. The MONA, on the other hand, shows a weak instability which can be cured by a single initialization step.

Example 2: An index-1 circuit with discontinuous sources. As a second example, we consider a full wave rectifier, see Figure 3, which is one of the classical components in electric and electronic devices used, for example, in an AC-DC converters. The purpose of this circuit is rectification of the input voltage denoted by the v_{src}. Thus, the main quantity of interest is the rectified voltage at the load modeled by the resistor R and denoted by v_{out}.

In the present example, the topology of the circuit is described by the following partial incidence matrices

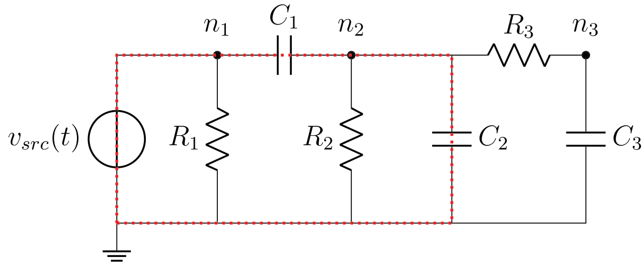

FIGURE 1 Index-2 circuit example from Figure 10.2 of Günther et al[4] containing a CV-loop marked with red dots

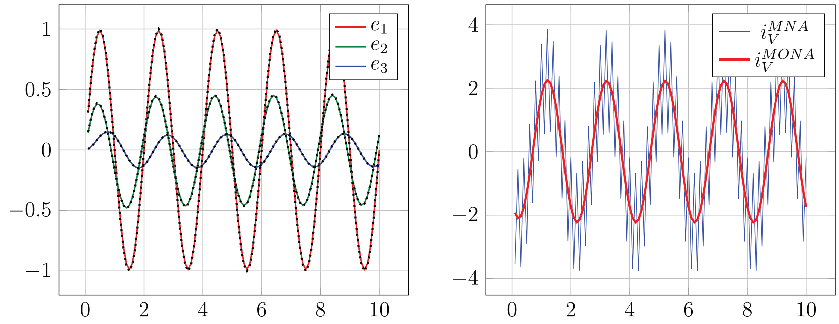

FIGURE 2 Numerical solutions obtained by the trapezoidal rule applied to the MNA and MONA formulations. Left: potentials (MNA: dotted; MONA: solid); right: current through voltage source

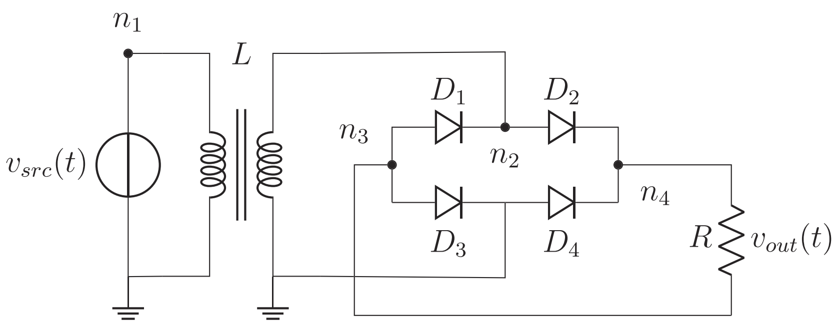

FIGURE 3 Schematic sketch of a full wave rectifier

$$A_L = \begin{pmatrix} 1 & 0 \\ 0 & 1 \\ 0 & 0 \\ 0 & 0 \end{pmatrix}, \quad A_R = \begin{pmatrix} 0 & 0 & 0 & 0 & 0 \\ -1 & 1 & 0 & 0 & 0 \\ 1 & 0 & 1 & 0 & -1 \\ 0 & -1 & 0 & -1 & 1 \end{pmatrix} \text{ and } A_V = \begin{pmatrix} 1 \\ 0 \\ 0 \\ 0 \end{pmatrix}$$

The circuit contains four diodes, which are modeled as resistors with a nonlinear voltage-current relation $j_D = 2.5(\exp(4v_D)+1)$ corresponding to the Shockley diode model. The nonlinear conductance matrix is then defined as

$$\begin{aligned} G:\ & \mathbb{R}^5 \to \mathbb{R}^5 \\ & v_i \mapsto j_D(v_i),\ i = 1, \ldots, 4, \\ & v_5 \mapsto v_5/R. \end{aligned}$$

For simplicity, we choose $R = 1$ for the remaining resistor. Like in Waltrich et al,[34] the magnetic coupling through the transformer is modeled by the inductance matrix

$$L = \begin{pmatrix} L_1 & K_{12} \\ K_{12} & L_2 \end{pmatrix} = \begin{pmatrix} 27.46 & 27.57 \\ 27.57 & 27.75 \end{pmatrix} \cdot 10^{-6}.$$

The conventianal MNA formulation here leads to an index-1 system which reads

$$\begin{pmatrix} 0 & 0 & 0 \\ 0 & L & 0 \\ 0 & 0 & 0 \end{pmatrix} \frac{d}{dt} \begin{pmatrix} e \\ i_L \\ i_V \end{pmatrix} + \begin{pmatrix} A_R G({A_R}^T e) {A_R}^T & A_L & A_V \\ -A_L^T & 0 & 0 \\ -A_V^T & 0 & 0 \end{pmatrix} \begin{pmatrix} e \\ i_L \\ i_V \end{pmatrix} = \begin{pmatrix} 0 \\ 0 \\ -v_{src}(t) \end{pmatrix}$$

and the MONA formulation yields a corresponding index-0 problem given by

$$\begin{pmatrix} A_R G\left(A_R{}^T \frac{d}{dt}\psi\right) A_R{}^T & A_V \\ -A_V^T & 0 \end{pmatrix} \frac{d}{dt}\begin{pmatrix} \psi \\ q_V \end{pmatrix} + \begin{pmatrix} A_L L^{-1} A_L^T & 0 \\ 0 & 0 \end{pmatrix}\begin{pmatrix} \psi \\ q_V \end{pmatrix} = \begin{pmatrix} 0 \\ -v_{src}(t) \end{pmatrix}.$$

Like in the previous test case, we used the trapezoidal rule with a fixed time step $\tau = 0.1$. For solving the nonlinear systems arising in each time step, we employed Newton's method with tolerance 10^{-10} and the solution of the previous time step as initial guess. In the top row of Figure 4, we display the rectified voltage v_{out} for a smooth input $v_{src}(t) = \sin(\pi t)$, which is consistent with trivial initial conditions. Both formulations are perfectly stable and yield second order convergence. In the second row of Figure 4, we display the corresponding results for the non-smooth digital input $v_{src} = \text{sign}(\sin(\pi t))$. Similar to an inconsistent initial condition, the discontinuities in the source term lead to a weak instability in the MNA formulation. The MONA system, on the other hand, which here is an ordinary differential equation, is not affected by the discontinuities in the source term.

Example 3: A larger test circuit. In our third example, we illustrate the applicability to larger problems and briefly comment on the choice of consistent initial values. As a test case, we consider the circuit illustrated in Figure 5. For our computations, the model parameters are set to $C_i = 1$ for $i = 1, \ldots, 9$ and $R_j = L_j = 1$ for $j = 1, \ldots, 7$, while the mutual inductances for the coupled coil pairs are chosen as $K_{14} = K_{25} = K_{36} = 0.1$. The voltage sources are prescribed as $v_{src,1}(t) = \sin(4t) + \cos(2t)$ and $v_{src,2}(t) = \sin(3t) + \cos(t)$.

This circuit represents a special case where both MNA and MONA formulations are of index-1. For MONA, this follows directly from Theorem 1, since (A1) holds but (A2) is not satisfied. From the assertions of Lemma 1, we further deduce that the MNA formulation is of index ≤ 2. Note that the circuit here contains *CV*-loops consisting of capacitors only, in which case one can still show that it is of index-1; see Estévez Schwarz and Tischendorf[25] for details.

Construction of consistent initial values. We use this example to also discuss the consistent choice of initial conditions. By transformation to Hessenberg form, which can be achieved by algebraic manipulations, the differential and algebraic components of the solution and the equations can be separated. Then initial conditions for the differential variables can be prescribed freely, while the starting values for the algebraic variables are obtained by solving the algebraic equation. For the problem under consideration, both formulations lead to a linear time-invariant DAE system

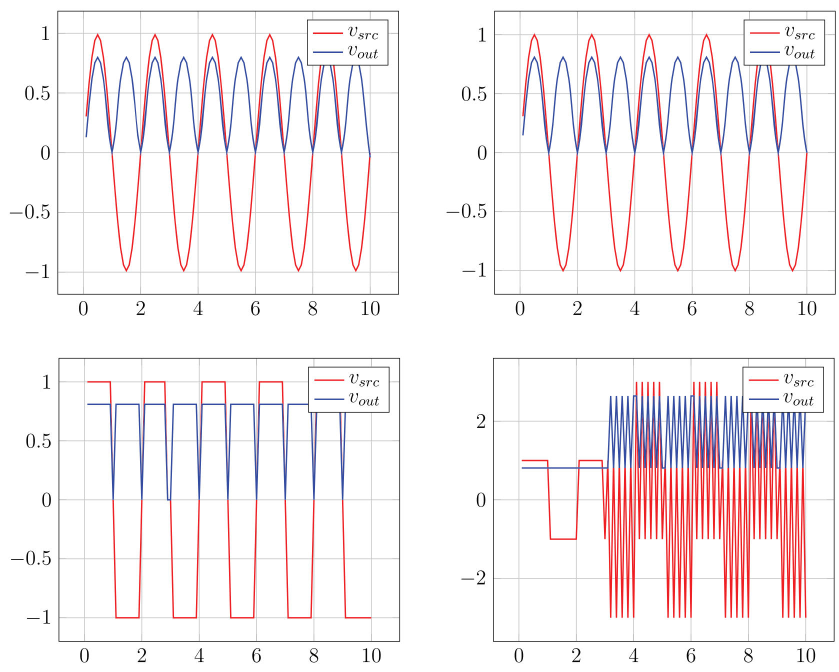

FIGURE 4 Numerical solutions for the AC-DC converter depicted in Figure 3 obtained with the trapezoidal. Top: $v_{scr} = \sin(\pi t)$; bottom: $v_{scr} = \text{sign}(\sin(\pi t))$; left: MONA; right: MNA

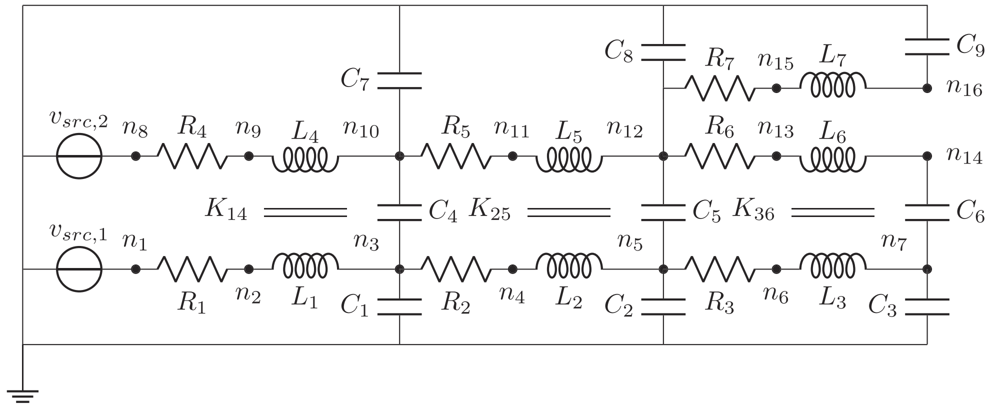

FIGURE 5 Test circuit from Shi et al.[35] (Section 10.2)

$E\frac{d}{dt}x + Ax = f$ of index $\nu = 1$ and the transformation to Hessenberg form can simply be realized using the singular value decomposition of the matrix E. For nonlinear systems arising from the MONA formulation, the transformation was carried out explicitly in the proof of Theorem 1. A similar projection-based analysis can done for nonlinear MNA systems; see, for example, previous studies.[36] In Estévez Schwarz,[37] an alternative step-by-step construction of initial values for MNA systems was presented based on topological arguments. This circumvents the computation of the singular value decomposition, which may become prohibitive for very large circuits.

For our numerical tests, we set the differential variables to zero at initial time, and compute the algebraic variables as described above. For the MNA formulation, the number of unknowns is 25, with 14 differential and 11 algebraic. Proceeding as described above, we get $e_1(0) = e_2(0) = 1$ and $e_8(0) = e_9(0) = -1$, while all other initial values are zero. The MONA formulation here leads to a system with a total of 27 unknowns, 25 of which are differential and only 2 are algebraic. Again, all differential variables are set to zero at initial time. Solving the algebraic constraints shows that also the remaining initial values should be chosen zero here.

Numerical results. In Figure 6, we compare the numerical solutions obtained by the trapezoidal rule with fixed time step $\tau = 0.1$. As mentioned above, both formulations here lead to an index-1 system, and after consistent specification of initial values, both methods perform very similar and lead to almost identical results.

6 | DISCUSSIONS AND OPEN TOPICS

In this paper we proposed a novel magnetic oriented formulation for electrical circuits, called MONA, which is based on magnetic node potentials and charges across capacitors as the primary unknowns. In contrast to that, standard approaches, like the conventional MNA and charge-flux based variants of it, use electric node potential and some of the branch currents and thus take an electric oriented viewpoint. Despite the different modeling perspective, MONA is applicable to the same general class of circuits and leads to a regular systems of differential-algebraic equations under the same topological conditions as required for MNA. Based on the particular geometric structure, passivity can again be established under general conditions on the device characteristics.

While the MNA yields an index $\nu \leq 2$ for admissible circuits, we could prove that MONA leads to an index $\nu \leq 1$, and apart from exceptional cases, the index of MONA is strictly smaller than that of MNA. Since the numerical difficulty of solving DAEs, in general, increases with the index,[23,24] this may be considered a key benefit of the MONA framework. Note that MONA is not based on an index-reduction of MNA, but is a completely different modeling approach. Another advantage of MONA is that fluxes and charges are directly accessible. On the other hand, electric quantities, like the node potentials and branch currents, have to be determined by differentiation, which seems to be disadvantageous. If Runge-Kutta collocation methods are used for time integration, this information is directly available and full convergence orders are retained.

The general algebraic structure of the linear or nonlinear systems that have to be solved in every time step are rather similar for MNA and MONA, but not the same. While MNA requires additional variables for the currents through inductors, MONA uses additional charges across capacitors. Therefore, the system size of MONA is larger than that of

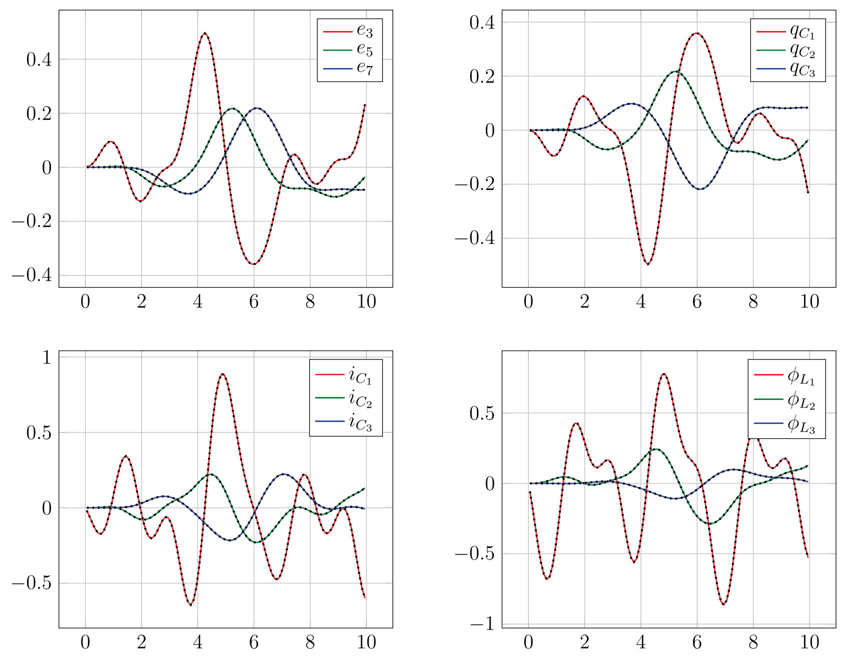

FIGURE 6 Comparison of numerical solutions of MNA (dotted) and MONA (solid)

MNA, if there are many capacitors but only few inductors. However, for circuits with many inductors and few capacitors, MONA leads to smaller systems than MNA. For VLSI circuits, both formulations require the iterated solution of large, typically sparse linear systems. State of the art algorithms are discussed, for example, in previous studies.[35,38,39] In summary, the computational effort for solving MNA and MONA formulations is very similar.

Conventional MNA in general leads to nonlinear dynamical systems of a dissipative Hamiltonian structure; also see Günther et al[18] for charge-flux based variants. Following Egger,[29] a passivity preserving time discretization can then always be achieved by discontinuous Galerkin methods. In contrast to that, MONA leads to systems with a generalized gradient structure and Petrov-Galerkin schemes or variants thereof should be used for a structure preserving discretization.[30,31]

The focus of this paper was on proposing MONA as an alternative modeling framework for electric circuits and establishing a complete index analysis. Before closing, let us also mention some topics for future research: Symbolic analysis has been applied successfully for MNA formulations of electric circuits.[35,40] In principle, the extension of such approaches to MONA seems possible but yet to be investigated. Also the incorporation of complex devices, like transistors, switches, etc. should be considered. Another aspect is the efficient computation of consistent initial conditions. Similar as in the context of MNA, we expect that this can again be done based on topological arguments,[37] thus avoiding the computation singular value decompositions which may become prohibitive for very large circuits. We expect that the smaller index $\nu \leq 1$ of MONA may actually simplify the constructions.

The magnetic oriented viewpoint can also be applied to derive a corresponding *magnetic oriented loop analysis* (MOLA). Details will be worked out in a forthcoming publication. Such magnetic oriented formulations seem particularly well-suited for the formulation of discretized magneto-quasistatic and equivalent circuit models applied in electric machine simulation and their coupling to electric power-supply circuits. Further field-circuit coupled problems arise when considering thermal effects.[41] The application of the MONA framework in this context is again yet to be considered.

ACKNOWLEDGMENTS

The support by the German Science Foundation (DFG) and the Austrian Science Fund (FWF) via grants TRR 361 and SFB F90-N, subproject C01 and C02, and by the Center for Computational Engineering at TU Darmstadt is gratefully acknowledged. Open access funding enabled and organized by Projekt DEAL.

DATA AVAILABILITY STATEMENT

Data sharing is not applicable to this article as no datasets were generated or analyzed during the study.

ORCID

Vsevolod Shashkov https://orcid.org/0000-0003-2677-9617
Idoia Cortes Garcia https://orcid.org/0000-0001-6557-103X

REFERENCES

1. Campbell S, Ilchmann A, Mehrmann V, Reis T. *Applications of Differential-Algebraic Equations: Examples and Benchmarks*: Springer; 2019.
2. Chua LO, Desoer CA, Kuh ES. *Linear and nonlinear circuits*. New York: McGraw-Hill; 1987.
3. Günther M, Feldmann U. The DAE-index in electric circuit simulation. *Math Comput Sim*. 1995;39:573-582.
4. Günther M, Feldmann U, ter Maten J. Modelling and discretization of circuit problems. *Handbook of Numerical Analysis*. Vol. 13. Elsevier; 2005:523-659.
5. Amrhein M, Krein PT. 3-d magnetic equivalent circuit framework for modeling electromechanical devices. *IEEE Trans Energy Conversion*. 2009;24:397-405.
6. Laithwaite ER. Magnetic equivalent circuits for electrical machines. In: Proceedings of the Institution of Electrical Engineers, Vol. 114; 1967:1805-1809.
7. Ruehli AE. Equivalent circuit models for three-dimensional multiconductor systems. *IEEE Trans Microw Theory Tech*. 1974;22:216-221.
8. Bannenberg MWFM, Ciccazzo A, Günther M. Coupling of model order reduction and multirate techniques for coupled dynamical systems. *Appl Math Lettr*. 2021;112:106780.
9. Bartel A, Baumanns S, Schöps S. Structural analysis of electrical circuits including magnetoquasistatic devices. *Appl Numer Math*. 2011; 61:1257-1270.
10. Bartel A, Günther M. PDAEs in refined electrical network modeling. *SIAM Rev*. 2018;60:56-91.
11. Cortes Garcia I, De Gersem H, Schöps S. A structural analysis of field/circuit coupled problems based on a generalised circuit element. *Numer Algor*. 2020;83:373-394.
12. Tischendorf C. Coupled systems of differential algebraic and partial differential equations in circuit and device simulation. *Model Numer Anal*. 2003.
13. Ho C-W, Ruehli A, Brennan P. The modified nodal approach to network analysis. *IEEE Trans Circuits Syst*. 1975;22:504-509.
14. Riaza R. *Differential-Algebraic Systems: Analytical Aspects and Circuit Applications*: World Scientific; 2008.
15. Riaza R, Torres-Ramírez J. Non-linear circuit modelling via nodal methods. *Int J Circ Theor Appl*. 2005;33:281-305.
16. Reis T. Mathematical modeling and analysis of nonlinear time-invariant RLC circuits. *Large-scale networks in engineering and life sciences*: Springer; 2014:125-198.
17. Gernandt H, Haller FE, Reis T, van der Schaft A. Port-Hamiltonian formulation of nonlinear electrical circuits. *J Geom Phys*. 2021;159: 103959.
18. Günther M, Bartel A, Jacob B, Reis T. Dynamic iteration schemes and port-Hamiltonian formulation in coupled differential-algebraic equation circuit simulation. *Int J Circuit Theory Appl*. 2021;49:430-452.
19. Scholz L. The signature method for daes arising in the modeling of electrical circuits. *J Comput Appl Math*. 2018;332:107-139.
20. Griepentrog E, März R. *Differential-algebraic equations and their numerical treatment*. Leipzig: Teubner; 1986.
21. Petzold L. Differential/algebraic equations are not ODE's. *SIAM J Sci Stat Comput*. 1982;3:367-384.
22. Brenan KE, Campbell SL, Petzold LR. *Numerical solution of initial-value problems in differential-algebraic equations*: SIAM; 1996.
23. Hairer E, Lubich C, Roche M. *The numerical solution of differential-algebraic systems by Runge-Kutta methods*: Springer; 2006.
24. Kunkel P, Mehrmann V. *Differential-algebraic equations*: European Mathematical Society (EMS), Zürich; 2006. Analysis and numerical solution.
25. Estévez Schwarz D, Tischendorf C. Structural analysis of electric circuits and consequences for MNA. *Int J Circuit Theory Appl*. 2000;28: 131-162.
26. Takamatsu M, Iwata S. Index characterization of differential–algebraic equations in hybrid analysis for circuit simulation. *Int J Circ Theor Appl*. 2010;38:419-440.
27. Tischendorf C. Topological index calculation of differential-algebraic equations in circuit simulation. *Surveys Math Indust*. 1999;8: 187-199.
28. Lamour R, März R, Tischendorf C. *Differential-Algebraic Equations: A Projector Based Analysis*. Berlin: Springer; 2013.
29. Egger H. Structure preserving approximation of dissipative evolution problems. *Numer Math*. 2019;143:85-106.
30. Egger H, Habrich O, Shashkov V. On the energy stable approximation of Hamiltonian and gradient systems. *Comput Meth Appl Math*. 2021;21(2):335-349.
31. Hairer E, Lubich C. Energy-diminishing integration of gradient systems. *IMA J Numer Anal*. 2014;34:452-461.
32. Nedialkov N, Pryce JD, Scholz L. An energy-based, always index ≤ 1 and structurally amenable electrical circuit model. arXiv: 210805106; 2021.

33. Brezzi F. On the existence, uniqueness and approximation of saddle-point problems arising from Lagrangian multipliers. *RAIRO*. 1974;8: 129-151.
34. Waltrich G, Duarte JL, Hendrix MAM. Multiport converters for fast chargers of electrical vehicles-focus on high-frequency coaxial transformers. In: The 2010 International Power Electronics Conference-ECCE ASIA-; 2010:3151-3157.
35. Shi G, Tan SX-D, Tlelo Cuautle E. *Advanced Symbolic Analysis for VLSI Systems*: Springer Science+Business Media New York; 2014.
36. Estévez Schwarz D, Lamour R. The computation of consistent initial values for nonlinear index-2 differential–algebraic equations. *Numer Algo*. 2001;26:49-75.
37. Estévez Schwarz D. A step-by-step approach to compute a consistent initialization for the MNA. *Int J Circ Theor Appl*. 2002;30:1-16.
38. Davis TA, Palamadai Natarajan E. Algorithm 907: KLU, a direct sparse solver for circuit simulation problems. *ACM Trans Math Softw (TOMS)*. 2010;37(3):1-17.
39. Reißig G. Fill reduction techniques for circuit simulation. *Electr Eng*. 2007;90(2):143-146.
40. Shi G. An analog circuit analysis method by node elimination. *Analog Integr Circ Sig Process*. 2021;109:247-252.
41. Tan SX-D, Amrouch H, Kim T, Sun Z, Cook C, Henkel J. Recent advances in EM and BTI induced reliability modeling, analysis and optimization (invited). *VLSI J Integr*. 2018;60:132-152.

How to cite this article: Shashkov V, Cortes Garcia I, Egger H. MONA—A magnetic oriented nodal analysis for electric circuits. *Int J Circ Theor Appl*. 2022;50(9):2997-3012. doi:10.1002/cta.3301